

November 21, 2017

Inclusive $t\bar{t}$ cross-section measurements at LHCRICHARD HAWKINGS¹*CERN, EP department, CH-1211 Geneva 23, Switzerland*

A review of ATLAS and CMS measurements of the inclusive $t\bar{t}$ production cross-section in pp collisions at $\sqrt{s} = 7\text{--}13$ TeV is presented, focusing on the most precise results in the dilepton and lepton+jets final states. The measurements are in good agreement with state-of-the-art QCD predictions, and have been used to determine the top quark pole mass and provide constraints on proton parton distribution functions.

PRESENTED AT

10th International Workshop on Top Quark Physics
Braga, Portugal, September 18–22, 2017

¹On behalf of the ATLAS and CMS Collaborations

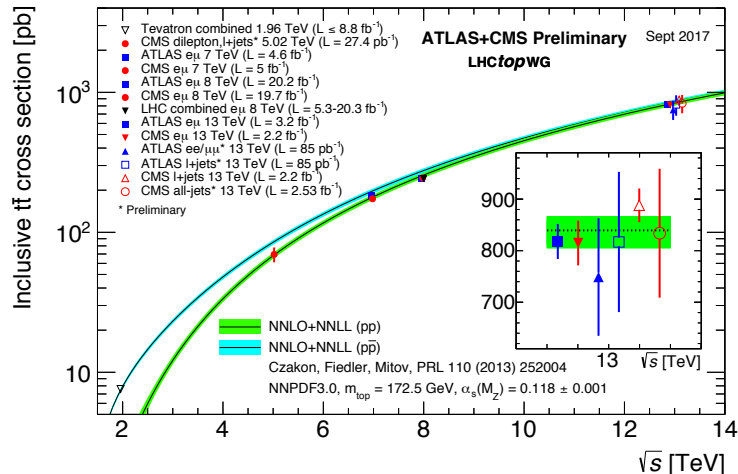


Figure 1: Selected LHC and Tevatron $t\bar{t}$ cross-section measurements as a function of \sqrt{s} compared to NNLO+NNLL QCD predictions [4].

1 Introduction

The inclusive top-pair ($t\bar{t}$) production cross-section $\sigma(t\bar{t})$ is an important quantity for characterising pp collisions in the TeV energy regime. At typical LHC energies ($\sqrt{s} = 7\text{--}13$ TeV), $t\bar{t}$ production is dominated by gluon fusion. It has been calculated to next-to-next-to-leading-order (NNLO) precision with resummation of next-to-next-to-leading-logarithmic (NNLL) soft gluon terms [1]. The uncertainties on the predictions for $\sigma(t\bar{t})$ at a fixed top quark mass of $m_t = 172.5$ GeV are around 5%, dominated by parton distribution function (PDF) and QCD scale uncertainties. The predicted cross-section also decreases by 3% for a 1 GeV increase in m_t .

The most precise measurements of $\sigma(t\bar{t})$ from the ATLAS [2] and CMS [3] experiments make use of the dilepton ($t\bar{t} \rightarrow \ell^+\ell^-\nu\bar{\nu}b\bar{b}$) and lepton+jets ($t\bar{t} \rightarrow \ell^\pm\nu q\bar{q}b\bar{b}$) channels, where both W bosons or just one decay to an electron or muon (denoted ℓ) and a neutrino. Less precise measurements in the all-hadronic channel and in final states involving hadronically-decaying τ -leptons have also been reported. The measurements are in good agreement with the predictions at all energies, as shown in Figure 1; when also including Tevatron results in $p\bar{p}$ collisions at $\sqrt{s} = 1.96$ TeV, the comparison spans two orders of magnitude in $\sigma(t\bar{t})$.

2 Measurement techniques

The cleanest measurements have been made in the dilepton channel with one electron and one muon, thereby suppressing the background from $Z \rightarrow \ell\ell$ +jets with two same-flavour leptons. The remaining background is dominated by $Wt \rightarrow e\mu+(b)$ jets events at the level of 3–10% depending on the selection. The CMS $\sqrt{s} = 13$ TeV analysis [5] selected events with at least two jets (at least one being b -tagged), and determined

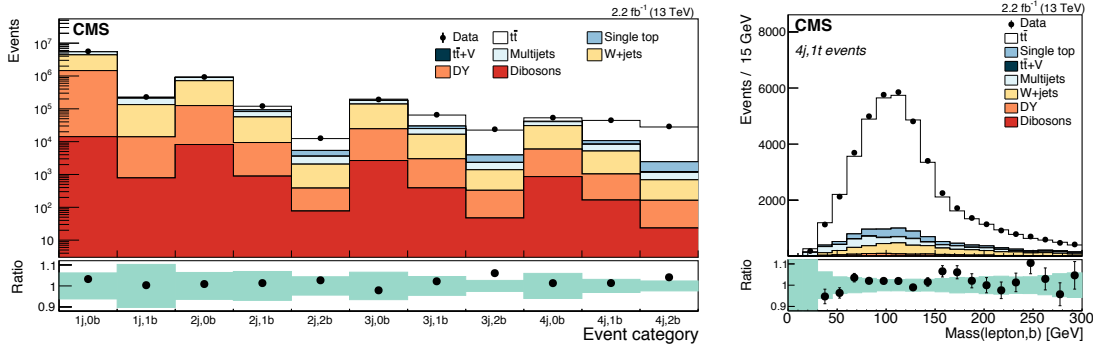


Figure 2: Event yields in various jet/ b -tagged jet multiplicity categories (left) and invariant mass of the lepton and b -tagged jet (right) for four jet/one b -tag events in the CMS lepton+jets analysis at $\sqrt{s} = 13$ TeV [10].

$\sigma(t\bar{t})$ from the yield of events after background subtraction. The resulting systematic uncertainties due to modelling of light jet production in $t\bar{t}$ events, jet energy scale and b -tagging efficiency were reduced in the ATLAS analyses at 7, 8 and 13 TeV [6, 7] by focusing on b -tagged jets only, and fitting simultaneously $\sigma(t\bar{t})$ and the probability to reconstruct and tag a b -jet from the top decay, from the rates of events with one and two b -tagged jets. The 7–8 TeV CMS analysis [8] went one step further, also using the zero b -tag events, and fitting the untagged jet multiplicity and jet transverse momentum distributions to constrain systematic uncertainties.

The lepton+jets channel offers larger statistics but brings significant additional backgrounds from t -channel single top, W +jet and QCD multijet production, that are typically estimated using data-driven techniques. The latest ATLAS $\sqrt{s} = 8$ TeV analysis [9] used the reconstructed two-jet invariant mass peak from the hadronic $W \rightarrow q\bar{q}$ decay and the rates of events with different jet and b -tagged jet multiplicities to reduce the jet energy scale and b -tagging uncertainties. It also made use of data $Z \rightarrow \ell\ell$ +jets events with one lepton transformed into a neutrino, in order to better model the W +jets background. The $\sqrt{s} = 13$ TeV CMS analysis [10] used a fit to all events with a lepton, significant missing transverse momentum and at least one jet, and categorised them according to jet and b -tagged jet multiplicity. As shown in Figure 2, the low multiplicity bins are dominated by backgrounds, allowing their normalisation to be determined from a fit, which also made use of a discriminating distribution (*e.g.* the invariant mass of the lepton and b -tagged jet) in each multiplicity category. The relative contributions of each event source in each category and bin were described by templates, with the effects of systematic uncertainties on these templates from detector and physics modelling effects being accounted for via auxiliary fit (‘nuisance’) parameters. The large number of fit categories with varying signal contributions allowed these parameters to be strongly constrained by the data, under the assumption that the model correctly captures all the sources of systematic uncertainty and their correlations across different bins and distributions.

| \sqrt{s} (TeV) | $\int L$ (fb ⁻¹) | Analysis | Stat. (%) | $t\bar{t}$ mod. (%) | Det. (%) | Bkg. (%) | Lumi. (%) | Total (%) |
|---------------------|---------------------------------|------------------------|--------------|------------------------|-------------|-------------|--------------|--------------|
| 13 | 3.2 | ATLAS $\ell\ell$ [7] | 0.9 | 3.0 | 1.1 | 0.9 | 2.3 | 4.1 |
| 13 | 2.2 | CMS $\ell\ell$ [5] | 1.0 | 2.4 | 3.6 | 1.5 | 2.3 | 5.3 |
| 13 | 2.2 | CMS ℓ +jets [10] | 0.2 | 1.7 | 2.3 | 1.9 | 2.3 | 3.8 |
| 8 | 20.2 | ATLAS $\ell\ell$ [6] | 0.7 | 1.7 | 1.2 | 0.9 | 2.1 | 3.2 |
| 8 | 19.7 | CMS $\ell\ell$ [8] | 0.6 | 1.3 | 2.2 | 1.5 | 2.6 | 3.7 |
| 8 | 20.2 | ATLAS ℓ +jets [9] | 0.3 | 4.1 | 2.3 | 1.3 | 1.9 | 5.7 |
| 8 | 19.6 | CMS ℓ +jets [11] | 1.6 | 5.4 | 2.5 | 0.2 | 2.6 | 6.5 |

Table 1: Comparison of fractional uncertainties due to data statistics, $t\bar{t}$ modelling, detector effects, background modelling and integrated luminosity, and the total uncertainty, for the most precise $\sigma(t\bar{t})$ measurements at $\sqrt{s} = 8$ and 13 TeV.

3 Comparison of uncertainties

The fractional uncertainties of the most precise dilepton and lepton+jets measurements at $\sqrt{s} = 8$ and 13 TeV are compared in Table 1, classifying the uncertainties reported in the original publications into various categories. The LHC beam energy-related uncertainties quoted in Ref. [6, 7] have been neglected, given that the beam energy has now been determined to a precision of 0.1% [12], corresponding to an effect of 0.2–0.3% on $\sigma(t\bar{t})$.

At $\sqrt{s} = 8$ TeV, dilepton measurements have the smallest uncertainties, with lepton+jets results suffering in particular from larger $t\bar{t}$ modelling uncertainties. At 13 TeV, the early dilepton results have significantly larger uncertainties than at 7–8 TeV, which should be reducible once the results of Monte Carlo tuning studies based on 13 TeV data are fully incorporated, and the lepton efficiencies, energy scales and resolutions are fully characterised using the copious $Z \rightarrow \ell\ell$ data. The most precise 13 TeV result to date comes from CMS in the lepton+jets channel [10], and benefits from the strong reduction in $t\bar{t}$ modelling uncertainties due to the in-situ constraints from the fit, to a much greater degree than in previous 7–8 TeV results.

4 Interpretation and outlook

The theoretical predictions for $\sigma(t\bar{t})$ are dependent on the top quark pole mass m_t^{pole} , a well-defined mass definition corresponding to that of a free particle, without some of the ambiguities inherent in reconstructing m_t from its decay products in a hadron collider environment. Some of the precise $\sigma(t\bar{t})$ measurements have therefore been interpreted as measurements of m_t^{pole} , as summarised in Table 2. Here, it is important to take into account the residual dependence of the measured $\sigma(t\bar{t})$ on m_t through $t\bar{t}$

| \sqrt{s} (TeV) | Analysis | PDF set | m_t^{pole} (GeV) |
|------------------|-----------------------|---------------|---------------------------|
| 7+8 | ATLAS $\ell\ell$ [6] | PDF4LHC Run-1 | $172.9^{+2.5}_{-2.6}$ |
| 7+8 | CMS $\ell\ell$ [8] | NNPDF3.0 | $173.8^{+1.7}_{-1.8}$ |
| 7+8 | CMS $\ell\ell$ [8] | MMHT2014 | $174.1^{+1.8}_{-2.0}$ |
| 7+8 | CMS $\ell\ell$ [8] | CT14 | $174.3^{+2.1}_{-2.2}$ |
| 13 | CMS ℓ +jets [10] | CT14 | 170.6 ± 2.7 |

Table 2: Measurements of the top quark pole mass m_t^{pole} from the inclusive $t\bar{t}$ production cross-section $\sigma(t\bar{t})$ for various datasets and PDF choices.

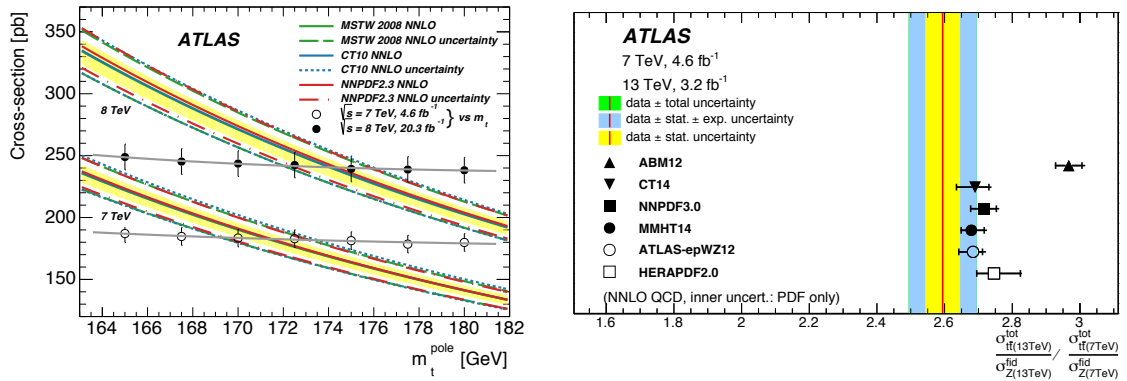


Figure 3: Comparison of ATLAS $\sqrt{s} = 7$ and 8 TeV measurements of $\sigma(t\bar{t})$ vs. assumed m_t with NNLO+NNLL predictions for various PDF sets [6] (left); measured double ratios of $t\bar{t}$ and $Z \rightarrow \ell\ell$ cross-sections at $\sqrt{s} = 13$ and 7 TeV compared to predictions from various PDF sets [13] (right).

acceptance and single top-quark production background (see Figure 3 (left)). This technique can reach a precision of about ± 2 GeV, driven mainly by PDF-related uncertainties on the predictions. It is important to use PDFs based on datasets which do not include $t\bar{t}$ production data to avoid potential circularity (the determination based on NNPDF3.0 in Table 2 has the smallest uncertainties, but NNPDF3.0 includes some constraints based on earlier LHC $\sigma(t\bar{t})$ measurements). The CMS measurements also treat the QCD scale uncertainties on the predictions with a uniform prior distribution, whereas ATLAS uses a more conservative Gaussian distribution.

Predictions for ratios of $t\bar{t}$ cross-sections $R(A/B)$ at different \sqrt{s} values A and B benefit from significant uncertainty cancellations, *e.g.* $R(8/7)$ is predicted to be 1.430 ± 0.013 . Some systematics also cancel in the experimentally-measured ratios, especially for measurements performed with the same technique at different \sqrt{s} values. The most precise measurement is currently $R(8/7) = 1.328 \pm 0.047$ [6], 2.1σ below the prediction and with an uncertainty dominated by the uncertainties on the integrated luminosities, which are only weakly correlated between the 7 and 8 TeV samples. Other $R(8/7)$ results [8, 11] and first ratios including $\sqrt{s} = 13$ TeV data [13] are

in good agreement with the predictions. Smaller uncertainties can be achieved by forming double-ratios of $t\bar{t}$ and Z -boson cross-sections at different energies, where the normalisation via the Z exchanges the luminosity uncertainty for a dependence on the quark/anti-quark PDF uncertainties which drive the Z cross-section predictions. First measurements of double ratios involving $\sqrt{s} = 13$ TeV data (Figure 3 (right)) show some sensitivity to PDFs, but would benefit from improved 13 TeV $t\bar{t}$ results with precision matching those at 7–8 TeV.

In conclusion, the measurements of $t\bar{t}$ inclusive cross-sections at LHC are now quite mature, with several precise (3–4%) results at $\sqrt{s} = 7$ –8 TeV from both ATLAS and CMS. Further improvements can be expected at 13 TeV with the use of larger datasets and refined analyses, and the first limited-precision measurement at 5 TeV [14] with 27 pb^{-1} should be followed-up using the larger dataset from 2017. The results to date are generally in good agreement with the predictions from NNLO+NNLL QCD, and have been used to constrain PDFs and determine the top quark pole mass.

References

- [1] M. Czakon and A. Mitov, *Comp. Phys. Comm.* 185 (2014) 2930, arXiv:1112.5675.
- [2] ATLAS Collaboration, *JINST* 3 (2008) S08003.
- [3] CMS Collaboration, *JINST* 3 (2008) S08004.
- [4] ATLAS+CMS top physics combined summary plots
<https://atlas.web.cern.ch/Atlas/GROUPS/PHYSICS/CombinedSummaryPlots/TOP/>.
- [5] CMS Collaboration, *Eur. Phys. J. C* 77 (2017) 172, arXiv:1611.04040.
- [6] ATLAS Collaboration, *Eur. Phys. J. C* 73 (2014) 3109, arXiv:1406.5375;
Addendum *Eur. Phys. J. C* 76 (2016) 642.
- [7] ATLAS Collaboration, *Phys. Lett. B* 761 (2016) 136, arXiv:1606.02699.
- [8] CMS Collaboration, *JHEP* 08 (2016) 029, arXiv:1603.02303.
- [9] ATLAS Collaboration, ATLAS-CONF-2017-054.
- [10] CMS Collaboration, *JHEP* 09 (2017) 051, arXiv:1701.06228.
- [11] CMS Collaboration, *Eur. Phys. J. C* 77 (2017) 15, arXiv:1602.09024.
- [12] E. Todesco and J. Wenninger, *Phys. Rev. Accel. Beams* 20 (2017) 081003.
- [13] ATLAS Collaboration, *JHEP* 02 (2017) 117, arXiv:1612.03636.
- [14] CMS Collaboration, arXiv:1711.03143.